Quantification of X3 absorption for ITER L-mode parameters in ASDEX Upgrade

Jörg Stober[1,*], *Martin* Schubert[1], *Mireille* Schneider[2], *Severin S.* Denk[3], *Rainer* Fischer[1], *Emanuele* Poli[1], *Dirk* Stieglitz[1], *Matthias* Willensdorfer[1], *Alberto* Loarte[2], *Daria* Ricci[4], ASDEX Upgrade Team[5], and Eurofusion MST-1 Team[6]

[1]Max-Planck-Institut für Plasmaphysik, Garching, Germany
[2]ITER Organization, St. Paul lez Durance, France
[3]Plasma Science and Fusion Center, Massachusetts Institute of Technology, Cambridge, USA
[4]Istituto per la Scienza e tecnologia dei Plasmi, Consiglio Nazionale delle Ricerche, Milano, Italy
[5]author list of *H. Meyer et al.* 2019 Nucl. Fusion **59** 112014
[6]author list of *B. Labit et al.* 2019 Nucl. Fusion **59** 086020

Abstract. For an early H-mode access in hydrogen, ITER considers operating at 1/3 of the full field using 170 GHz X-Mode for heating at the 3^{rd} harmonic. The optical thickness for such a heating scheme depends on T_e^2. It is rather low in the ohmic phase (with T_e about 1-2 keV), but reaches high single pass absorption for the strongly EC heated plasma with T_e exceeding 10 keV. Launching ECRH into an ohmic plasma may trigger a boot-strap process on T_e if the additional power absorption due to increasing T_e exceeds the additional power losses due to increased transport (which often tends to increase with input power). In this contribution we present measurements of the X3 absorption for the parameter range relevant for ITER, i.e. $n_e \approx 2 \cdot 10^{19}\, m^{-3}$, $T_e \geq 2\, keV$ in order to back up theoretical estimates used for the modeling so far. In ASDEX Upgrade (AUG) such low densities cannot be reached in H-mode such that dominant heating with NBI is not an option. For moderate T_e, it is also not an option to use X3 heating as main heating, due to the excessive stray radiation threatening in-vessel components. This dilemma is solved with the 2-frequency EC system of AUG. The main central heating is done with the lower frequency of 105 GHz at the 2^{nd} harmonic and full single pass absorption. Up to 3.5 MW of ECRH are used at that frequency to vary T_e. Two other gyrotrons are used at 140 GHz to probe the X3 interaction close to the plasma center with a sequence of short blips. The expected values of single pass absorption are calculated with TORBEAM and vary from 7% to 70%. Below 40% single pass absorption the non-absorbed power triggers an arc in the tile gaps of the inner heat shield which screens the thermo-couples from the incoming beam such that they cannot be used. Between 40% and 80% single pass absorption, the predictions and measurements agree within the uncertainty of the measurement, unless we have clear evidence for non-linear interactions, which are not described by TORBEAM and which are not expected in ITER, but are due to some specific experimental choices for an isolated subset of our results.

1 X3-heating in ITER

The motivation for this work is given by the interest of ITER to operate early in its operational phase at 1/3 of the nominal magnetic field B in order to verify predictions on the L/H power threshold and to allow an early start of ELM studies and ELM control [2]. During the first phase of plasma operation called PFPO-1, only ECRH will be available for plasma heating. In order to avoid time consuming and costly changes to the EC system, operation at the third harmonic of the cyclotron frequency ω_{ce} is desirable ($B = 1.8\, T$). At full field ($B = 5.3\, T$), EC operates at the fundamental ω_{ce}. Since ω_{ce} drops linearly with B both scenarios can be run with the same EC frequency ($170\, GHz$). Only the polarization of the beam has to be adapted; X-mode at the third harmonic (X3) vs. O-mode for the fundamental (O1), but this is already available since X-mode heating at half field is also foreseen (X2).

The optical depth for X3 absorption is not necessarily much larger than unity [1]. Thus, incomplete single pass absorption and related machine damage have to be taken into account. X3 absorption increases strongly with T_e, giving potentially rise to a bootstrap process such that the initially only partially absorbed EC-heating generates a fully absorbing target mainly by rising T_e.

First modeling results for such scenarios for ITER are published in [3]. Figure 1 reproduces two figures of this publication. The top figure shows the rise of the central T_e after switching on $10 - 30\, MW$ of EC power at $275\, s$. The bottom part shows the corresponding decrease of the power not absorbed during the first path. Initially only 25% of the power is absorbed, increasing to close to 100% after a fraction of a second for $\geq 20\, MW$. The energy not absorbed during the first $300\, ms$ is about $150\, kJ$ per beam ($1\, MW$, 50% absorption, $0.3\, s$). In ASDEX Upgrade we have good experience with a limit of $80\, kJ$ non-absorbed power in short pulses (except for hitting windows

*e-mail: joerg.stober@ipp.mpg.de

directly), but the power density in the beam footprint in ITER is probably more than a factor of 2 lower, such that 150 kJ is a reasonable number. Still this exercise shows that the bootstrap process must not last significantly longer and it should reduce the non-absorbed power to only a few percent. The 10 MW case in fig 1 would not be acceptable for machine safety.

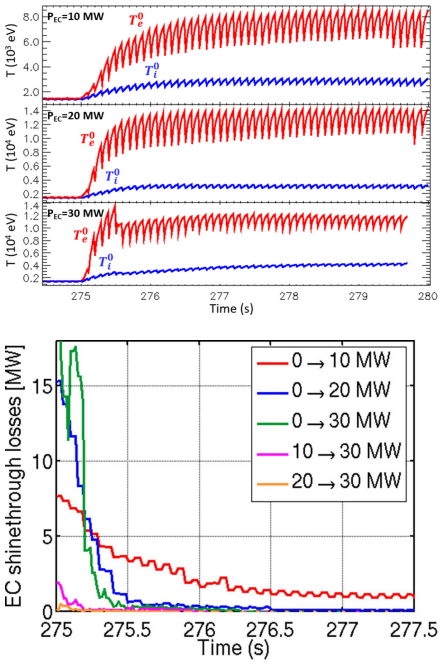

Figure 1. Modeling results for X3 heating in ITER from [3], figs. 6, 9. Top: evolution of central T_e, T_i after switching on 10 – 30 MW of ECRH. Bottom: evolution of the power not absorbed during the first path through the plasma.

Being close to the margin for machine safety raises concern on the accuracy of the model, which essentially has to balance the power densities absorbed from the microwave-beams (+ ohmic heating) for given n_e, T_e-profiles with transport effects describing how the kinetic profiles react on changes of the power profile. ITER has identified (1) the transport model and (2) the (linear)[1] absorption model as crucial elements and put this forward to the ITPA. For (1) the Transport and Confinement group was contacted. Results based significantly on EC heated discharges in AUG are published in [4]. For (2) the Integrated Operational Scenarios group was contacted and the work reported in this paper is a direct consequence.

2 X3 heating in ASDEX Upgrade

In AUG, X3 heating is used since more than a decade [5]. In contrast to the plans in ITER, the radial position of the resonance is chosen slightly on the low field side (LFS). This allows to have the X2 resonance still in the plasma on the high field side (HFS). Especially in H-modes this allows full absorption of the power not absorbed by the central X3 resonance. In fact, using EC in an ohmic plasma under these conditions, leads to an L/H-transition due to the power initially absorbed at the edge ([6], and references therein for more details on X3 usage). In cases when the X2 beam-dump is insufficient, holographic reflectors on the HFS may be used also for X3 (they were originally designed for O2 [5]). For 140 GHz, they maintain polarization and reflect and refocus the beam close to the plasma center. Since these reflectors are equipped with fast thermo-couples, the latter can be used to detect transmitted power as described during this workshop by *M. Schubert* [7]. Of course one has to lower B such that the X2 resonance is no longer absorbing power from the beam after it passed through the X3 resonance.

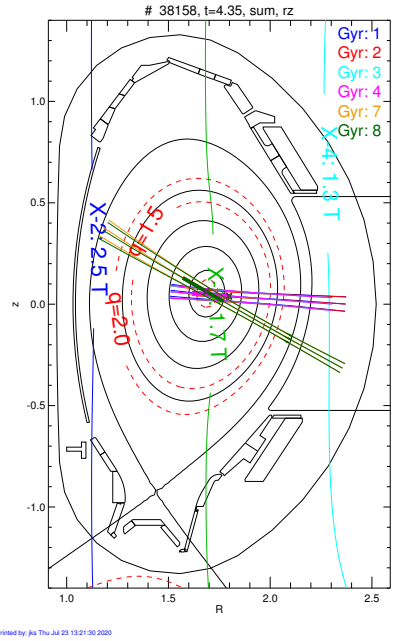

Figure 2. Initial setup for the EC system (poloidal projection): Beams 1-4 (horizontal) were tuned to 105 GHz, while beams 7,8, tuned to 140 GHz, target the thermo-couples on the upper HFS reflector tiles. $B_t = -1.7\,T$. The solidly colored areas along the beam path indicate where the majority of the power is deposited as calculated by TORBEAM. The cold resonances shown as blue and green lines correspond to 140 GHz. Note that in the later discharges (#39747-39751), beam 7 was replaced by beam 6.

To analyze scenarios with low single pass absorption, the X3 resonance itself is not suited for heating. This would be rather inefficient and dangerous for the machine. On the other hand, significant neutral beam injection drives the plasma into H-mode, such that the targeted ITER parameter range $10^{19}\,m^{-3} \leq n_e \leq 2 \cdot 10^{19}\,m^{-3}$ and $1.5\,keV \leq T_e \leq 6\,keV$ cannot be reached. A way out is to use a lower frequency EC beam to heat the plasma at the respective X2 resonance. Ideally this frequency would be 2/3 of the X3 probing frequency, Then the cold resonances would overlay. On AUG the gyrotrons are capable of 2 frequencies with the ratio 3/4 i.e. 105 GHz / 140 GHz (for details on the AUG EC system see [6]). In order to heat the plasma rather centrally with 105 GHz X2, and the 140 GHz X2 resonance being in the scrape-off layer on the

[1] See discussion in section 2.3.

HFS, one has to make use of the Doppler-term in the resonance condition and inject the 105 GHz beams with significant toroidal angle ($\approx$ 20°), i.e. with a large $N_{\|}$. These conditions can be realized for B between 1.6 T and 1.7 T. Figure 2 shows the situation for 1.7 T.

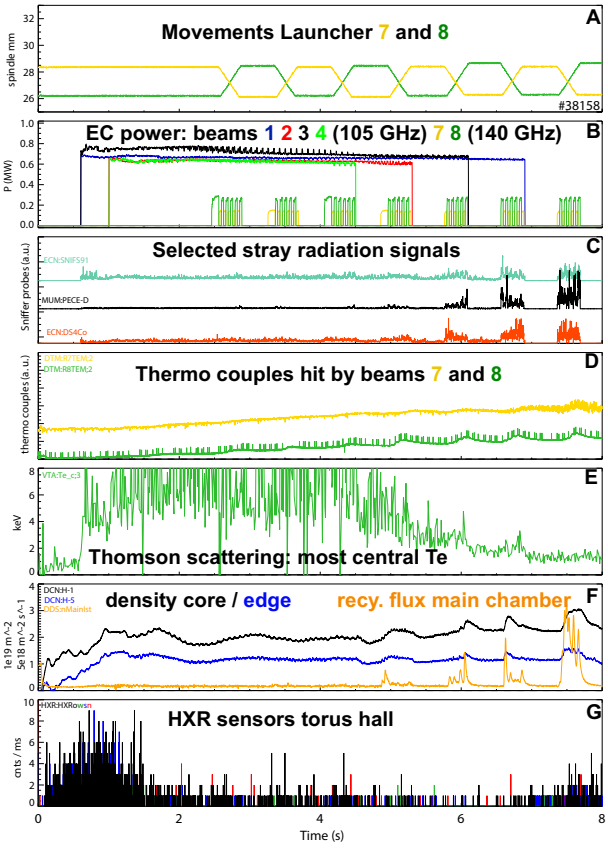

Figure 3. AUG #38158, I_p: 800 kA, B_t: -1.7 T. See text for detailed discussion.

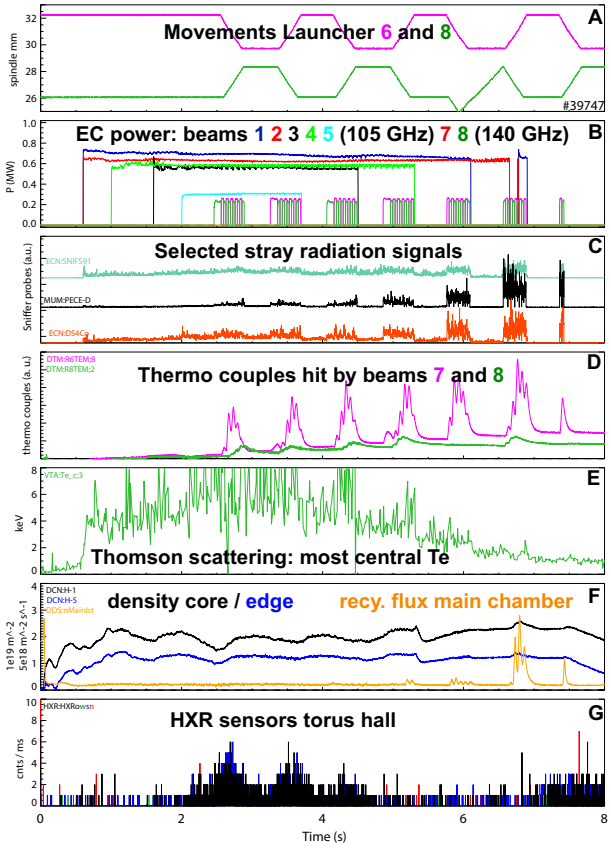

Figure 4. AUG #39747, I_p: 800 kA, B_t: -1.6 T. To ensure plasma initiation and to avoid locked-modes in the ramp-up phase the plasma was started with B_t: -1.7 T. The field was changed between 1.4-2.6 s. Otherwise identical control parameters as figure 3, except that beam 6 had to be used with 140 GHz since beam 7 was not available. The 105 GHz heating uses up to 5 beams (4 in fig. 3). As can be seen from box A, there was a mistake in programming the fifth sweep of launcher 8 in this specific discharge. Consequently, there is no rise of the TC on the respective reflector in box D.

2.1 X3 absorption experiments

The experiments were conducted as sketched above, resulting in 6 successful discharges of which two are shown in figures 3,4 performed on two days in July 2020 (#38158) and July 2021 (#39747-51). The experiments were conducted in hydrogen plasmas to avoid L/H transitions. On the days before the experiments the 140 GHz blips were injected into the empty vessel to fine-tune and fix the toroidal launching angles and to get the no-absorption level from the thermo-couples, using the same timing of launcher movements and 140 GHz blips as in the plasma experiments in the morning of the next day (figure3, boxes A,B). Five blips of 30 ms are applied while the beam is swept poloidally over the thermo couple. This allows to cope with slight variations of the refraction (essentially due to variations of the density peaking), in contrast to a static set-up. The toroidal variation of refraction is negligible according to TORBEAM [8]. For details of the analysis of the thermo-couple data see [7]. For higher expected absorption a longer pre-blip was applied in order to reach steady conditions during the phase of mirror movement. Also shown in box B are the traces for the 105 GHz beams. For the first 3 sweeps the power was constant (4 beams), then it decreased successively (3, 2, 1, 0 beams). Boxes C,D show the reaction of some stray-radiation-diodes and the thermo-couple (TC) data. The stray radiation increases significantly towards the end of the discharge, whereas the correlated rise of the TC-data seems to saturate. Box E shows that the variation of the 105 GHz power led to the expected variation of T_e, while n_e (Box F) was kept at the envisaged low values. The T_e data are determined from Thomson-Scattering (TS), since the stray radiation may damage the ECE. After determining the stray radiation levels, the sweeps with higher absorption were repeated with ECE, while those with lower absorption were repeated without the 140 GHz blips, but with ECE. Except for the cases with non-thermal electrons as discussed in section 2.2, ECE and TS agreed sufficiently well. Box G shows hard X-ray (HXR) data related to such relativistic electrons, and in figure 3 those are only found as a very small run-away population in the first sec. of the discharge. Also shown in box F is a trace of the recy-

cling flux in the main chamber measured with an ionization gauge. It is strikingly in phase with the latter sweeps and the amplitude of the sniffer signals. The increase of the recycling flux must be related to a particle source driven by a sufficiently high level of stray radiation. This is also obvious from the reaction of the line-integrated density signals on these fluxes. As indicated in figure 2 the non-absorbed power crosses the X2 resonance in the scrape-off layer on the HFS. One may speculate that due to the relatively short connection length to the wall an arc can be fed by the wave at that location, which would probably lead to increased hydrogen desorption and at the same time shield the TCs from a part of the non-absorbed power. The effect would likely increase with the non-absorbed power and would also need a minimum power level to ignite the arc.

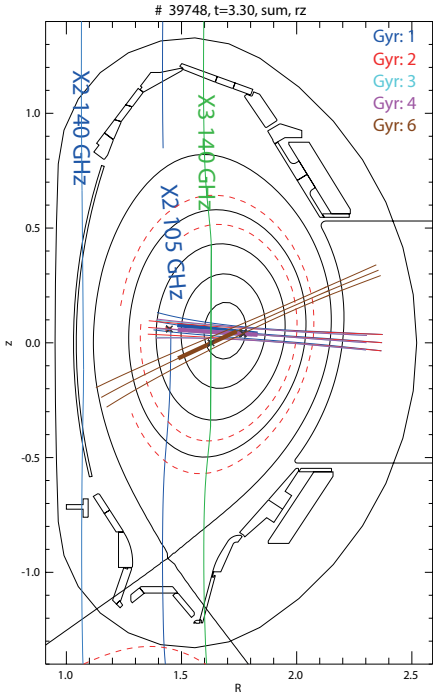

Figure 5. Beam propagation, cold resonances and regions of EC power deposition as calculated by TORBEAM for #39748 at 3.3 s (i.e. beam 8 off), which is the pre-heating phase of the second sweep. The phase is similar as in #39747 except that beam 8 is off and ECE data are available. The T_e profiles used for the TORBEAM calculation are based on the LFS ECE channels (see discussion in section 2.2.

In the discharges from 2021 it was therefore attempted to lower B further to shift the X2 resonance into the reflector tile. Since gyrotron 7 was under repair, beam 6 and the respective reflector tile were used instead. As seen in box D of figure 4 the response of this TC was significantly stronger, probably due to poorer thermal connection during the mounting (see [7] for details). Again one finds that the sniffer signals show the expected increase in transmitted power as T_e drops, whereas the TCs do not show a significant change for the latter sweeps, for example sweep 4 and 6, i.e. the change of B_t did not suppress this effect. The reflector tile for beam 6 can be seen with the video diagnostic. For #39747 (fig. 4) light emission is observed close to the position of the TC for sweeps 3-7[2]. It is very week for sweep 3 and strongest for sweep 6. Sweep 7 was incomplete due to a soft stop related to the OH coil limit. This is a direct confirmation of a discharge glowing in the vicinity of the TC. For sweeps 4-7 fig. 4 F shows a clear reaction of the recycling flux, but only for the pulses with beam 8. In any case we expect that the power measured with the TCs will be reduced under these conditions. We note from figure 5 that the cold X2 resonance for the 140 GHz blips is for beam 6 still just in front of the reflector. For beam 8 ($z_{heat\ shield} \approx 0.5\,m$ as in fig. 2, beam not shown in fig. 5), it is in the tile, respectively in the gap. Apparently also a resonance in a gap can lead to a significant particle source. Maybe the solid surface next to the resonance leads to an efficient fueling (production of secondary electrons) for the arc.

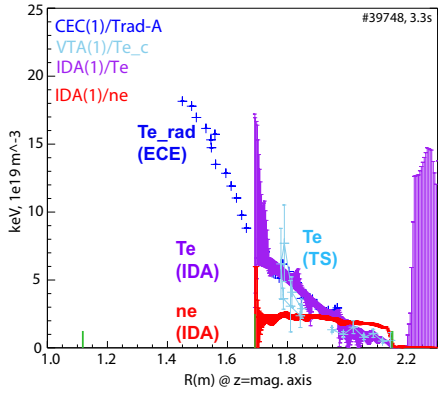

Figure 6. n_e and T_e profiles for AUG #39748 closest to 3.3s, no time averaging. T_e data from Thomson scattering (TS) and ECE-emission ($T_{e,rad}$). The integrated data analysis (IDA) used the low field side (LFS) ECE data for T_e and the interferometry and Lithium-beam data for n_e [9].

2.2 Non-thermal (non-linear) effects

As mentioned above, the discharges were repeated with the ECE diagnostic active (and no 140 GHz blips where high sniffer levels had been observed). In some cases the radiation temperature was found to rise strongly for channels on the HFS (figure 6). This was only observed for $B_t = 1.6\,T$ and $P_{105GHz} \geq 2.5\,MW$. It has been checked with the radiation transport code ECRad [10] in combination with integrated data analysis [9] if this could be explained by shine-through effects due to limited optical thickness, as it was found to explain large radiation temperatures at the LFS edge of some plasmas. Still, no sensible T_e-profiles were identified which would explain the data under these assumptions. Thus, one has to take non-thermal effects into consideration. Since the 2^{nd} harmonic ECE emission of fast particles is shifted to lower frequencies due to the relativistic mass increase of the electrons, this radiation should be reabsorbed by slower electrons at larger major radius R as the radiation travels to the LFS

[2]camera id 06Bul1, with low pass filter > 900 nm, same view with narrow H_α filter (id 06Bul) shows no obvious signal

where the detector is located. This means that the source of radiation must be located at larger R than the corresponding cold X2 resonance, such that the radiation can escape. 3^{rd} harmonic emission from electrons with a relativistic γ-factor of a bit lower than 3/2 in the center of the plasma would fulfill this condition. $\gamma \leq 3/2$ corresponds to a kinetic energy below half of the electron rest energy, i.e. $\leq$ 256 keV (faster ones would not be seen, again due to the X2 resonance.). Electrons in the energy range should be visible on the HXR data. shown in box G of figure 4. For the phases with 4 and 5 EC-beams with 105 GHz, the signal level is clearly elevated. We also see that the HXR signals increase further during X3 blips (140 GHz), indicating that fast electrons are further accelerated, in other words the presence of the non-thermal electrons influences the absorption of the X3-blip. In such cases the latter needs to be estimated taking the distortion of the electron distribution into account.

The fast electron population is generated by a specific combination of the magnetic field and the large $N_{\|}$ of the 105 GHz injection (in spite of the net current being almost balanced). Figure 5 shows that the absorption region is largely Doppler-shifted since the cold resonance is located on the HFS behind the peak of the (thermal) electron temperature. The large shift means that the EC accelerates electrons with initial energies well above kT. If B is larger, the cold resonance is closer to the plasma center and only electrons with a smaller parallel velocity are resonant in the plasma center, i.e. the heating goes more to the bulk of the electron distribution. This can be modeled with a code describing the collisional relaxation process, but as discussed in section 2.3 this is not the focus of this paper.

2.3 Comparison with linear theory

The non-thermal effects as described in the previous section are not expected to be relevant in ITER. The larger the machine, the better is the assumption, that an electron leaving an EC beam will thermalize before it re-enters another EC-beam. For the absorption calculation this allows to always assume a Maxwellian velocity-distribution. The absorption profile scales under those circumstances linearly with the input power, since no distortion builds up which would introduce a non-linearity by its dependence on input power. It is this kind of linear theory which was used in the calculations for fig. 1 and for which ITER is interested to test the validity. While in [3] the code GRAY was used, on AUG the code TORBEAM[8] is used. Both codes differ in the description of the Gaussian beam, but have been successfully bench marked for ITER [11]. In particular we set up TORBEAM to use the same absorption routine by *D.Farina*. Figure 7 compares the single pass absorption measured with the TCs to the calculation by TORBEAM. The fat blue crosses on the right correspond to the situations for which we expect the agreement to be good and indeed deviations are of the order of a few percent only. Red crosses indicate cases with non-thermal electrons, for which the TCs show higher single pass absorption than calculated with the linear code. This may be

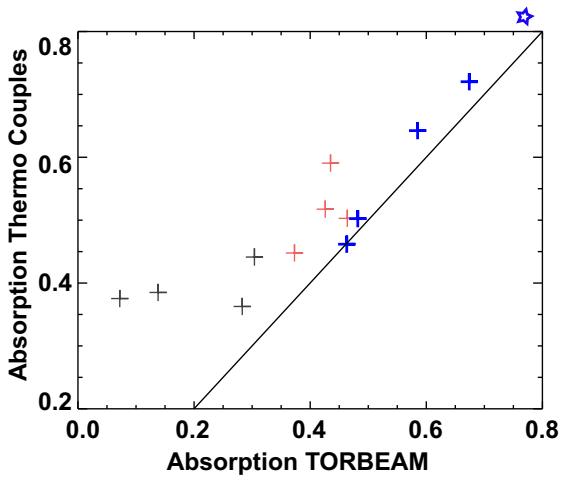

Figure 7. Comparison of the single-path absorption calculated by TORBEAM based on the n_e, T_e profiles determined with IDA to the single path absorption determined with the TCs. Grey crosses correspond to cases with increased main chamber recycling fluxes or light on the video from the reflector. Red crosses correspond to cases with increased HXR levels (here IDA used TS data for T_e). The blue crosses are the remaining undisturbed data. All data except the blue star are from beam 6, which has the most structured TC data, reducing the error in the power estimation. The blue star corresponds to an early analysis of the 2^{nd} and 3^{rd} sweep with beam 8 in fig. 3 (TS data still to be reanalyzed with all the modeling established meanwhile [7]). The point is added here, since it corresponds to the highest single pass absorption achieved in the described experiments.

expected since X3 absorption depends strongly on the Larmor radius, such that velocity distributions with excessive fast electrons may absorb more than calculated assuming a Maxwellian. Finally the gray crosses correspond to cases with additional recycling fluxes or light in front of the TC as described above. Here the TCs miss part of the transmitted power because the plasma in front does absorb it, thus the apparent single-pass absorption is higher. Apart from those caveats the linear theory describes well the observations, though for a more limited range of single pass absorption (or T_e) than originally envisaged.

3 Conclusions and Outlook

Within the experimental limitations the linear theory (here represented by TORBEAM) describes well the measured X3 single-pass absorption. Unfortunately, single-pass absorption below 40% could not be accessed, due to effects of the X2-resonance close or inside the gaps of the inner heat-shield leading to de-gassing and arc formation distorting the power measurement in the tile. All sniffer probes signals increase significantly as the single-pass absorption calculated by TORBEAM drops below 40% (figure 8, but also figures 3,4). Still a quantitative analysis is difficult. The sketched parabola corresponds to a direct reflection, i.e. if only one path would be followed in both directions through the plasma. Of course multiple reflections are also important especially at low absorption and more distant probes.

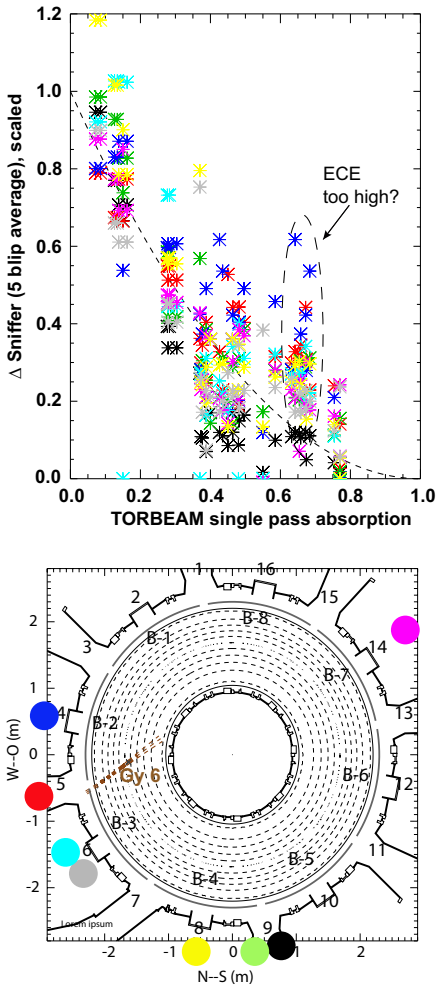

Figure 8. Top: Average increase of the sniffer signals for the five subsequent blips during the sweeps of beam 6 plotted against the single pass absorption calculated with TORBEAM. Some data appear twice: in case IDA T_e was significantly different with ECE and TS, two TORBEAM runs were made using the different T_e profiles. Most points in the vertically elongated dashed ellipse correspond to non-thermal electron distributions using ECE. The corresponding ones using TS lie at lower single.pas absorption (lower T_e, fig. 6). The sniffer increase was scaled with reference to the empty vessel reference.[a] The data is underlined with a parabola, see text. Bottom: Toroidal location of sniffer-probes and beam 6. Absolute values of more distant probes are lower, but this is hidden by the normalization as explained above.

[a] Additional scaling factors between 0.5 and 2.5 had to be introduced for the different probes, minimizing the scatter at the lowest and largest absorption and aiming at a value of unity for zero TORBEAM absorption. These factors were adjusted by eye. An explanation may be the lack of mode mixing by plasma fluctuations in the empty vessel, giving rise to less variable highly localized interference structures, no longer smeared out by time averages over the mode sensitive sniffers signals.

The appearance of the arcs on the HFS during these experiments may be avoided by reducing the beam power. Here the onset was observed when less than half the power was absorbed, suggesting a reduction of the gyrotron power by a factor of two will solve the issue, which may be technically still possible. Especially for ITER the lowest absorption levels may be relevant, since it is rather the T_e value than the absorption, which should be compared . The latter scales favorably for ITER with the ratio $(B/\nabla B)/\lambda_{EC}$, which is more than a factor of 4 larger in ITER than in AUG. The absorption of 25% mentioned above for the ohmic ITER plasma corresponds to 6% for a plasma with similar n_e, T_e in AUG, close to the lowest value in fig. 7 (7% for an ohmic plasma in AUG).

With respect to machine safety in ITER, the arcs observed in AUG on the HFS may trigger some analysis. Alternatively or as an initial test, ITER may envisage a regime with a HFS-X2-dump inside the plasma as referred to above for AUG. B_t of 2.0-2.1 T seems feasible to achieve that. The disadvantage would be a higher L/H-threshold and a limited use of the upper launcher. The latter would only be an issue if more than 24 gyrotrons were available, i.e. if the EC-system would be extended. Since X3-heating does essentially come without current drive, issues like MHD-(de)stabilization can anyway not be tested. Finally we note, that the non-linear cases observed in AUG are nicely diagnosed and a good test-case for Fokker-Planck codes.

Acknowledgment

The views and opinions expressed herein do not necessarily reflect those of the ITER Organization.
This work has been carried out within the framework of the EUROfusion Consortium, funded by the European Union via the Euratom Research and Training Programme (Grant Agreement No 101052200 — EUROfusion). Views and opinions expressed are however those of the author(s) only and do not necessarily reflect those of the European Union or the European Commission. Neither the European Union nor the European Commission can be held responsible for them.
S.S. Denk acknowledges support of his work by US DOE under DE-SC0016154.

References

[1] V. Erckmann and U. Gasparino, Plasma Phys. Control. Fusion **36**, 1869 (1994)
[2] ITER Organization, Tech. Rep. ITR-18-003 (2018), Appendix G, `https://www.iter.org/doc/www/content/com/Lists/ITER Technical Reports/Attachments/9/ITER_Research_Plan_within_the_Staged_Approach_levIII_provversion.pdf`
[3] M. Schneider et al., Nucl. Fusion **59**, 126014 (2019)
[4] C. Kiefer et al., Nucl. Fusion **61**, 066035 (2021)
[5] H. Höhnle et al., Nucl. Fusion **51**, 083013 (2011)
[6] J. Stober et al., Plasma Phys. Control. Fusion **62**, 024012 (2020)
[7] M. Schubert et al., *Experiments with reduced single pass absorption at ASDEX Upgrade – instrumentation and applications* (2022), these conference proceedings
[8] E. Poli et al., Computer Phys. Comm. **225**, 36 (2018)
[9] R. Fischer et al., Fusion Sci. Technol. **76**, 879 (2020)
[10] S. Denk et al., Computer Phys. Comm. **253**, 107175 (2020)
[11] M. Schneider et al., Nucl. Fusion **61**, 126058 (2021)